

Evolution of Cooperation for Multiple Mutant Configurations on All Regular Graphs with $N \leq 14$ players

Hendrik Richter
 HTWK Leipzig University of Applied Sciences
 Faculty of Engineering
 Postfach 301166, D-04251 Leipzig, Germany.
 Email: hendrik.richter@htwk-leipzig.de

November 12, 2019

Abstract

We study the emergence of cooperation in structured populations with any arrangement of cooperators and defectors on the evolutionary graph. Using structure coefficients defined for configurations describing such arrangements of any number of mutants, we provide results for weak selection to favor cooperation over defection on any regular graph with $N \leq 14$ vertices. Furthermore, the properties of graphs that particularly promote cooperation are analyzed. It is shown that the number of graph cycles of certain length is a good predictor for the values of the structure coefficient, and thus a tendency to favor cooperation. Another property of particularly cooperation-promoting regular graphs with a low degree is that they are structured to have blocks with clusters of mutants that are connected by cut vertices and/or hinge vertices.

1 Introduction

Describing conditions for the emergence of cooperation in structured populations is a fundamental problem in evolutionary game theory [4, 19, 20, 35]. In structured populations the network describing which players interact with each other may be crucial for the fixation of a strategy. Recently, several attempts have been made to explore the universe of interaction graphs in order to link graph properties to fixation. For a single cooperator this question has been studied intensively and recently relationships have been mapped for a large variety of different interaction graphs connecting which strategy is favored with the fixation probabilities and the fixation times [2, 18, 25, 32]. These results clarify for a single mutant the relationships between the graph structure, on the one hand, and fixation probability and fixation time, on the other. The main findings are that generally fixation probability and fixation time is correlated such that a higher fixation probability comes with a higher fixation time. Within this general rule, it has further been shown that generalized stars maximize fixation probability while minimizing fixation time, while comet-kites minimize fixation probability while maximizing fixation time [18]. Furthermore, if we allow self loops and weighted links, we may construct arbitrarily strong amplifiers of selection [25]. Compared with these findings, the problem of multiple cooperators (or more than one mutant) is far less studied. One approach uses configurations and

structure coefficients [6] and has shown that cooperation is favored over defection under conditions which can be linked to spectral graphs measures and cooperator path length [27, 28].

This study deals with strategy selection for multiple mutants on evolutionary graphs and addresses two central questions. The first is to find out which interaction network modeled as a regular graph yields the largest structure coefficient and therefore is most suited to promote the evolution of cooperation. This is reported for all regular graphs with $N \leq 14$ vertices (= players). This question is studied subject to three parameters, the number of players, coplayers and cooperators. Answering this question may inform designing interaction networks with prescribed abilities to promote or suppress cooperation. As there are some trends over varying these three parameters, it appears possible to conjecture for beyond the considered parameters. The second question studied takes up the observation that there are differences in the values of the structure coefficients over regular interaction graphs and asks what makes some graphs different from others in terms of promoting the evolution of cooperation. Our main interest is what these differences are from a graph-theoretical point of view. This goes along with identifying certain properties of regular cooperation-promoting graphs. The main result is that the number of graph cycles of certain length is a good predictor of a large value of the structure coefficient. Especially for a smaller number of coplayers graphs that particularly promote cooperation have rather cycles with small length. Furthermore, these graphs are structured to have blocks that are connected by cut vertices and/or hinge vertices. Cooperators cluster on these blocks and serve as a mutant family that may invade the remaining graph. The study presented here uses structure coefficients, which have been derived for birth-death and death-birth processes [6]. However, as the structure coefficients solely depend on the distribution of cooperators and defectors on the evolutionary graph, they could be, at least in principle, also calculated for other strategy updating processes as long as these processes are not completely random. Thus, the methodology reported here is also applicable for other types of non-imitative dynamics.

The paper is structured as follows. In Sec. 2 the main results are given. In particular, upper and lower bounds on the structure coefficients are presented for all interaction networks modelled as regular graphs with $N \leq 14$ players. Furthermore, it is shown that between maximal structure coefficients (and thus conditions favoring the prevalence of cooperation) and the count of cycles with certain length, there is an approximately linear relationship. The results are discussed in Sec. 3, while the Appendices review the methodological framework of configurations, regular graphs and structure coefficients, discuss graph isomorphism, and give a collection of graphs with maximal structure coefficients.

2 Evolution of Cooperation

2.1 Upper and lower bounds on the structure coefficients

The structure coefficient $\sigma(\pi, \mathcal{G})$ introduced by Chen et al. [6] (see [27, 28] for further analysis) is a measure of whether or not cooperation is favored over defection in games with any arrangement of cooperators and defectors on regular evolutionary graphs. More strictly speaking, in an evolutionary game with weak selection and a payoff matrix (4), the fixation probability of cooperation is larger than the fixation probability of defection if $\sigma(\pi, \mathcal{G})(a - d) > (c - b)$, see also Appendix 1. This condition connects the values of the payoff matrix, the structure of the evolutionary graph \mathcal{G} and the arrangement of cooperators and defectors on this graph expressed by the configuration π with long-term prevalence of cooperation. The structure coefficient $\sigma(\pi, \mathcal{G})$ generalizes the structure coefficient σ introduced by Tarnita et al. [31] which yields the same condition for favoring cooperation, $\sigma(a - d) > (c - b)$, but applies to a single cooperator (or a single mutant). By

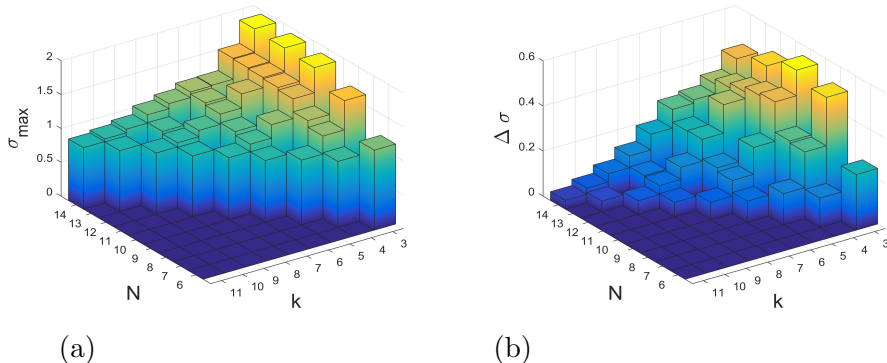


Figure 1: The maximal structure coefficient σ_{max} and the maximal difference $\Delta\sigma = \sigma_{max} - \sigma_{min}$ over the number of players N and coplayers k for all regular interaction graphs with $6 \leq N \leq 14$ and $3 \leq k \leq N - 3$ according to Tab. 2.

contrast, $\sigma(\pi, \mathcal{G})$ is valid for any arrangement of cooperators and defectors on the evolutionary graph and specifically for several cooperators (or multiple mutants).

As the structure coefficient varies over configurations π and graphs \mathcal{G} , it is natural to ask about upper and lower bounds of $\sigma(\pi, \mathcal{G})$. In this paper, we approach this question by checking all $\sigma(\pi, \mathcal{G})$, which appears feasible for a small number of players $N \leq 14$ and all regular graphs with up to 14 vertices. We classify the structure coefficients and graphs with respect to the number of players N . Furthermore, the configurations π are also grouped according to the number of cooperators $c(\pi)$, $2 \leq c(\pi) \leq N - 2$, while the graphs \mathcal{G} are sorted according to the number of coplayers k (which equals the degree of the graph). As the structure coefficients $\sigma(\pi, \mathcal{G})$ vary over configurations *and* graphs \mathcal{G} , we may define two bounds. A first is over all $2^N - 2$ non-absorbing configurations, which we call σ_{max_i} . Thus, we obtain for each graph \mathcal{G}_i , $i = 1, 2, \dots, \mathcal{L}_k(N)$, the quantity $\sigma_{max_i} = \max_{\pi} \sigma(\pi, \mathcal{G}_i)$. A second bound, called σ_{max} , is derived from the first bound and additionally collects over all $\mathcal{L}_k(N)$ regular graphs with a given N and k according to Tab. 2. Thus, we get $\sigma_{max} = \max_i \sigma_{max_i}$. For the minimum, the bounds are defined like-wise.

Fig. 1 shows the maximal structure coefficient σ_{max} and the maximal difference $\Delta\sigma = \sigma_{max} - \sigma_{min}$ over players N and coplayers k . As discussed in Appendix 2 these results apply to any instance of a regular graph, for example to random regular graphs. It can be seen that the maximal structure coefficient σ_{max} is largest for $k = 3$, which is cubic graphs. For $k > 3$, the values of σ_{max} get gradually smaller. In other words, the more coplayers there are, the smaller is σ_{max} . Also, for a constant number of coplayers, σ_{max} increases with N , which is the number of players. The increase, however, gets gradually smaller and converges for $N \rightarrow \infty$ to a constant, which is $\sigma(\pi, \mathcal{G}) \rightarrow \sigma = (k + 1)/(k - 1)$ [6, 21]. For instance, for $k = 3$, the structure coefficients converge to $\sigma(\pi, \mathcal{G}) \rightarrow \sigma = 2$. In other words, for the thermodynamic limit with an infinite population, prevalence of cooperation only depends on the number of coplayers k of a regular graph, but not on the graph structure or the number and arrangement of cooperators on the graph. The largest difference between maximal and minimal structure coefficient $\Delta\sigma = \sigma_{max} - \sigma_{min}$ we also get for $k = 3$. Here, $\Delta\sigma$ increase to a largest values (for instance for $k = 3$ this happens for $N = 10$) before falling for N getting even larger, converging to $\Delta\sigma = 0$ for $N \rightarrow \infty$.

We next analyze the maximal structure coefficients depending on the number of cooperators $c(\pi)$. Thus,

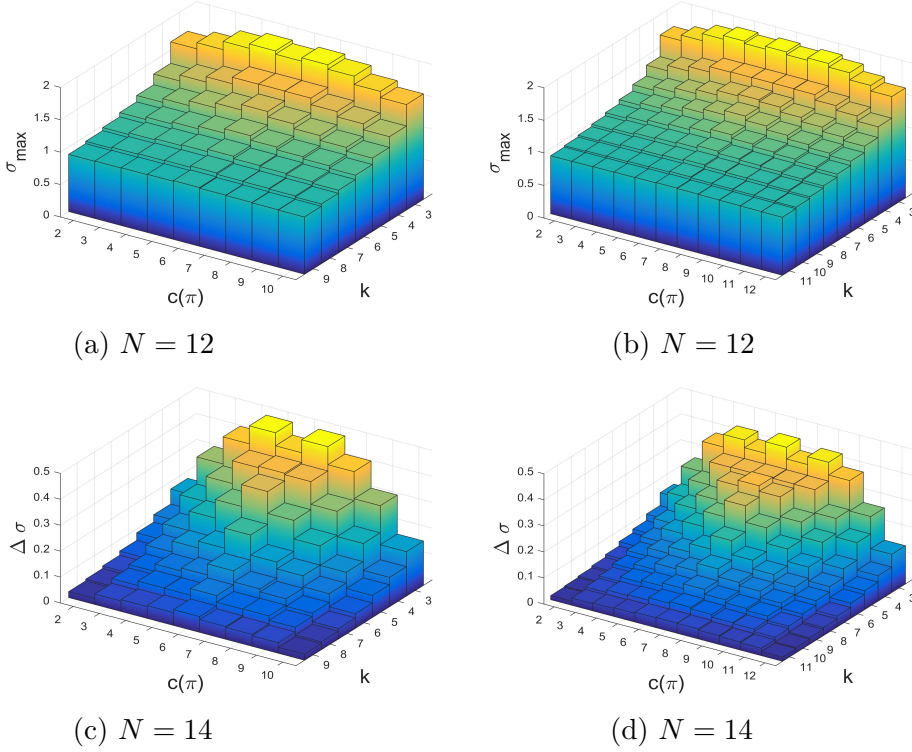


Figure 2: The maximal structure coefficient σ_{max} and the maximal difference $\Delta\sigma = \sigma_{max} - \sigma_{min}$ over the number of coplayers k and cooperators $c(\pi)$ for all regular interaction graphs with $N = 12$ and $N = 14$ according to Tab. 2.

the maximum is over all $\#_{c(\pi)} = \binom{N}{c(\pi)}$ configurations with the same number of cooperators $2 \leq c(\pi) \leq N-2$ and all regular graphs according to Tab. 2. The maximal values of σ_{max} and $\Delta\sigma$ are obtained for $c(\pi) = N/2$ for N even and for both $(N+1)/2$ and $(N-1)/2$ for N odd. An exception is $N = 12$ and $k = 3$, where σ_{max} is obtained for $c(\pi) = 5$ and $c(\pi) = 7$. Furthermore, we get the following results, see Fig. 2 as examples for $N = 12$ and $N = 14$. The value σ_{max} and $\Delta\sigma$ are symmetric with the number of cooperators $c(\pi)$ and generally higher for the number of cooperators and defectors exactly or approximately the same than for a small number of cooperators or a small number of defectors. For the number of coplayers k getting larger, the differences over the number of cooperators $c(\pi)$ for both σ_{max} and $\Delta\sigma$ are levelled.

Apart from the numerical values of the maximal structure coefficients σ_{max} and their relations to the number of players N , coplayers k and cooperators $c(\pi)$, it is also interesting to know for which of the $\mathcal{L}_k(N)$ graphs the maximal values occurs. We call the graphs for which this happens the σ_{max} -graphs. Their number is $\#\sigma_{max}$. Tab. 1 give the number of σ_{max} -graphs, $\#\sigma_{max}$, for all N and k considered here, see also Appendix 3 for some examples of σ_{max} -graphs. If we compare these numbers with the total number $\mathcal{L}_k(N)$ of k -regular graphs on N vertices, see Tab. 2, we observe that $\mathcal{L}_k(N)$ grows much faster than $\#\sigma_{max}$. In other words, the σ_{max} -graphs become rare as N increases. Fig. 3 shows the quantity $\#_{log} = -\frac{1}{N^2} \log \left(\frac{\#\sigma_{max}}{(4k-1/4k^2)\mathcal{L}_k(N)} \right)$ over N and k (Fig. 3a), and over $c(\pi)$ and k for $N = 14$ (Fig. 3b). We

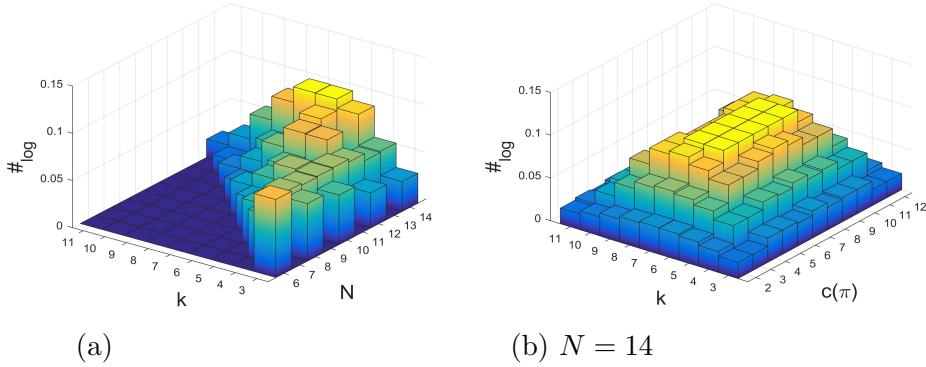


Figure 3: The quantity $\#_{\log} = -\frac{1}{N^2} \log \left(\frac{\#\sigma_{max}}{(4k-1/4k^2)\mathcal{L}_k(N)} \right)$ relating the number of σ_{max} -graphs, $\#\sigma_{max}$, to the number of regular graphs $\mathcal{L}_k(N)$ for players N , coplayers k and cooperators $c(\pi)$

Table 1: The numbers $\#\sigma_{max}$ of graphs with maximal σ_{max} for all regular graphs with $\mathcal{L}_k(N) > 1$ and $6 \leq N \leq 14$.

$k \setminus N$	6	7	8	9	10	11	12	13	14
3	1	0	1	0	1	0	4	0	10
4	0	2	1	1	1	1	2	10	14
5	0	0	2	0	1	0	1	0	1
6	0	0	0	3	2	5	1	2	1
7	0	0	0	0	2	0	4	0	1
8	0	0	0	0	0	5	6	49	4
9	0	0	0	0	0	0	4	0	14
10	0	0	0	0	0	0	0	7	14
11	0	0	0	0	0	0	0	0	4

may conclude that as a rough approximation the ratio $\frac{\#\sigma_{max}}{\mathcal{L}_k(N)}$ falls exponentially in N and polynomially in k for $k \approx N/2$ and N getting larger. Furthermore, observe from Fig. 3b that for small and large values of the number of cooperators $c(\pi)$ there is a larger number of graphs that are σ_{max} -graphs. The σ_{max} -graphs become rarer for $c(\pi) \approx N/2$, for which but σ_{max} is largest.

2.2 Relationships between structure coefficients and graph cycles

Recently, Giscard et al. [7] proposed an algorithm to count efficiently the number of cycles with length ℓ in a graph: $\mathcal{C}_\ell(N, k)$ with $3 \leq \ell \leq N$. Thus, it is feasible to count $\mathcal{C}_\ell(N, k)$ for all $\mathcal{L}_k(N)$ regular graphs with $N \leq 14$, as given in Tab. 2. As an example see Fig. 7 with the count $\mathcal{C}_\ell(6, 3)$, $\ell = \{3, 4, 5, 6\}$, for the $\mathcal{L}_3(6) = 2$ graphs with $N = 6$ and $k = 3$. The following discussion is based on taking into account these numerical results.

In the previous section, it was shown that the maximal structure coefficients vary over interaction networks modelled as regular graphs, even if the number of players, coplayers and cooperators is constant.

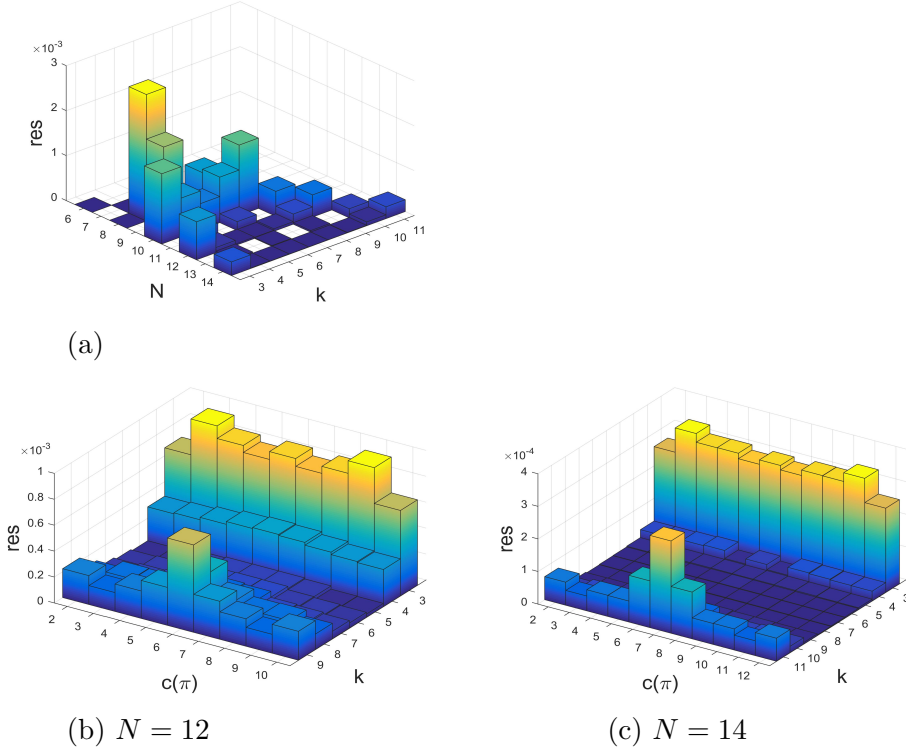


Figure 4: Residual error res according to Eq. (1) over N , k and $c(\pi)$.

Thus, it appears reasonable to assume that some features of the graphs may be associated with these differences. In the following, results are presented in support for an approximately linear relationship between the number of graph cycles with certain length and the maximal structure coefficients. Two previous results can be interpreted as to point at the validity of such a relationship between the number of graph cycles and fixation properties. A first is from evolutionary games on lattice grids [8, 9, 14, 23]. For these games, it has been shown that clusters of cooperators have a higher fixation probability than cooperators that are widely distributed on the grid. The location of the cluster on the grid does not matter. As lattice grids can be described by regular graphs (a Von Neumann neighborhood is a 4-regular graph, a Moore neighborhood a 8-regular graph) clusters imply short and closed paths between the nodes of the grid. Furthermore, the grid means an abundance of cycles with even cycle length. A second result is that between the structure coefficients and the path length between the cooperators there is a strong negative correlation [28]. Cooperator path length is defined as the path length averaged over all pairs of cooperators on the evolutionary graph. If there are more than two cooperators, the cooperator path length has particularly small values if the cooperators cluster next to each other and are linked by loops. Thus, small values of the cooperator path length correspond with the abundance of cycles of certain length.

As there are $\mathcal{L}_k(N)$ regular graphs for a given N and k , we obtain $\mathcal{L}_k(N)$ maximal structure coefficients σ_{max_i} , $i = 1, 2, \dots, \mathcal{L}_k(N)$ together with the same count of cycle length $\mathcal{C}_{\ell_i}(N, k)$. Thus, we may assume for each i a linear relationship $\sigma_{max_i} = \mathcal{C}_{\ell_i}(N, k)x + \epsilon_i$ for some variables x with an error term ϵ_i . To test the

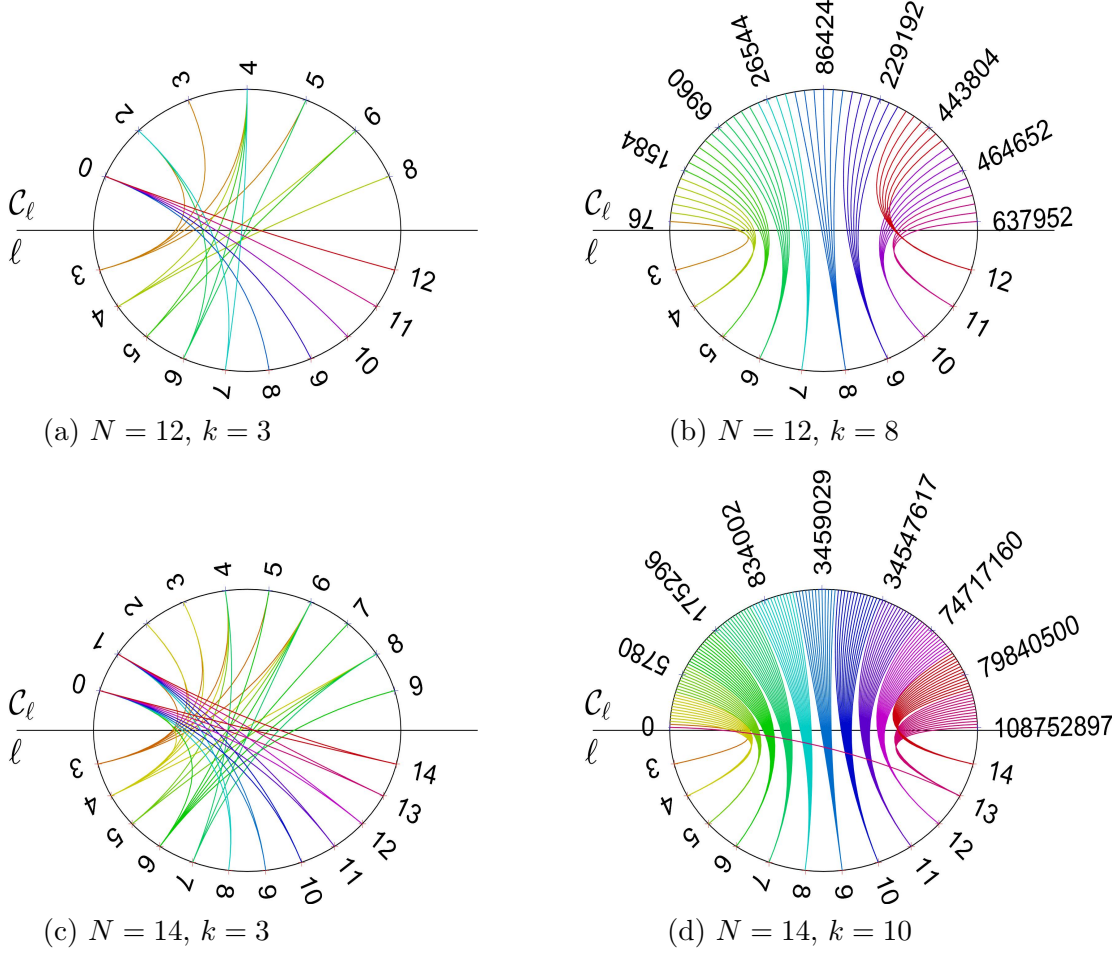


Figure 5: Examples of schemaballs of σ_{max} -graphs.

validity of this linear relationship, we calculate the residual error

$$\text{res} = \frac{1}{\mathcal{L}_k(N)} \|\mathcal{C}_\ell x^* - \sigma_{max}\|, \quad (1)$$

where \mathcal{C}_ℓ comprises of all $\mathcal{L}_k(N)$ cycle length $\mathcal{C}_{\ell_i}(N, k)$ and σ_{max} contains all $\mathcal{L}_k(N)$ structure coefficients σ_{max_i} for a given N and k . The variable x^* is the solution of the non-negative least square problem

$$x^* = \arg \min_x \|\mathcal{C}_\ell x - \sigma_{max}\|. \quad (2)$$

As the length of x^* varies with varying $\mathcal{L}_k(N)$, the residual error in (1) is weighted by $\mathcal{L}_k(N)$ to make it comparable over all N and k . Note that the residual error (1) gives equivalent results to the root-mean-square deviation, which is also sometimes used to measure the accuracy of a (linear) model. The results are given in Fig. 4. We see that the residual error res is small for all $6 \leq N \leq 14$, $3 \leq k \leq N - 3$ and

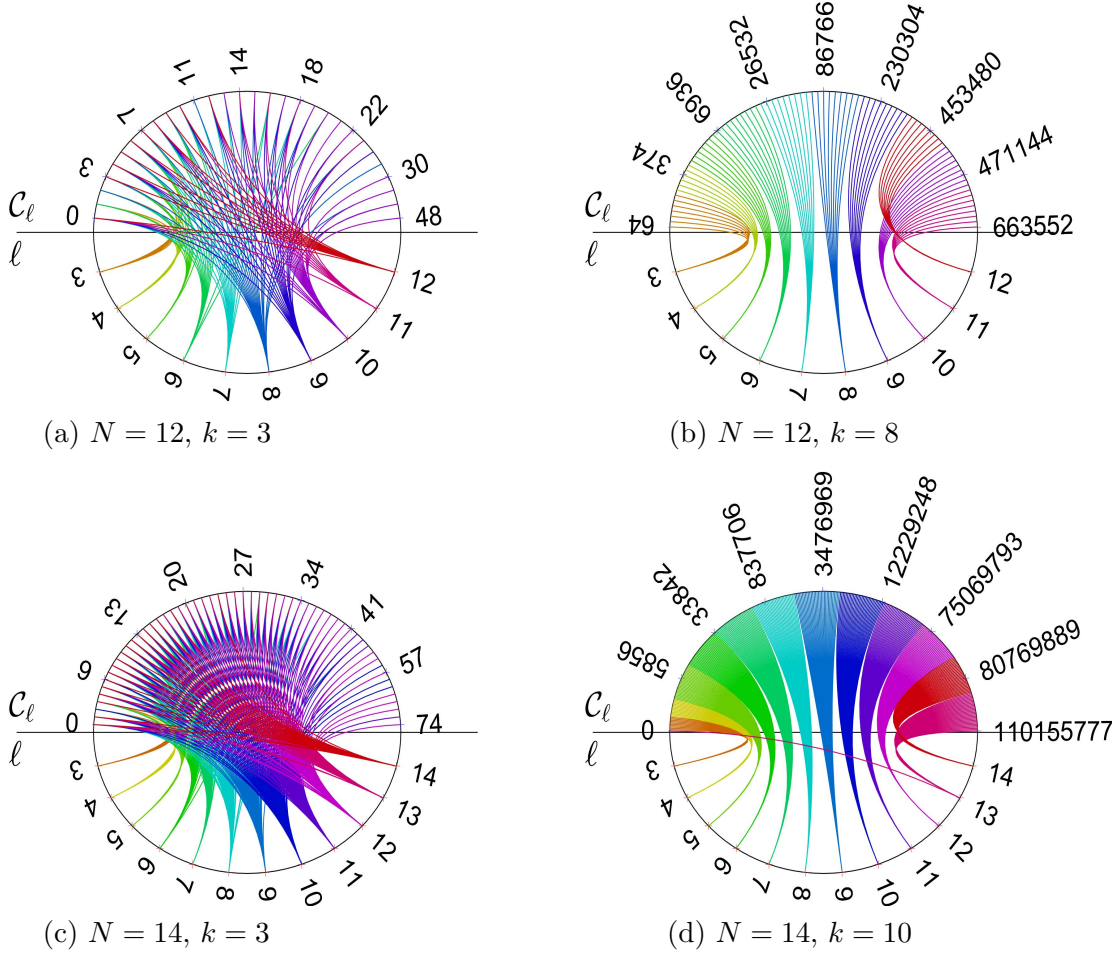


Figure 6: Examples of schemaball of σ_{min} -graphs.

gets even smaller for N getting larger. Generally, the error res is slightly larger for $k = 3$ and $k = N - 3$ than for intermediate values of k . This is also true for calculating res for each number of cooperators $c(\pi)$, see Figs. 4b and 4c, which show the results for $N = 12$ and $N = 14$. For $N = 14$ the values of res are generally smaller than for $N = 12$ and the largest values of res are obtained for small and large k for all $c(\pi)$. To conclude we can observe that the results for the residual error res are generally very small, which is equivalent to saying that the error term ϵ_i in the assumed linear relationship $\sigma_{max_i} = \mathcal{C}_{\ell_i}(N, k)x + \epsilon_i$ has an expected value $\mathbb{E}(\epsilon_i) \approx 0$. Thus, there is some justification to observe that between the maximal structure coefficients σ_{max_i} and the cycle count $\mathcal{C}_{\ell_i}(N, k)$ there is an approximately linear relationship.

Finally, another aspect of the interplay between graph structure and fixation properties should be highlighted. To begin with, we analyze the cycle count $\mathcal{C}_{\ell}(N, k)$ of σ_{max} -graphs, which are those graphs among the $\mathcal{L}_k(N)$ regular graphs that have maximal structure coefficients. Consider the example $N = 12$ and $k = 3$. There are $\mathcal{L}_3(12) = 85$ graphs of which $\#\sigma_{max} = 4$ are σ_{max} -graphs, compare Tab. 1 with Tab. 2. For these 4 graphs we analyze how the count $\mathcal{C}_{\ell}(12, 3)$ is distributed over $\ell = 3, 4, \dots, 12$. A possible way

to visualize such an analysis is based on schemaballs [13, 27], see Fig. 5a. In such a schemaball we draw Bezier curves connecting the count $\mathcal{C}_\ell(N, k)$ in the upper half of the ball with the associated cycle length ℓ in the lower half. The actual values of both ℓ and $\mathcal{C}_\ell(N, k)$ are written on the ball. The curves are colored in such a way that equal values of the cycle length ℓ have the same (and specific) color, no matter to which cycle count $\mathcal{C}_\ell(N, k)$ they are belonging. The colors are selected equidistant from a RGB color wheel. If there are several σ_{max} -graphs, as there are $\#\sigma_{max} = 4$ for $N = 12, k = 3$ in Fig. 5a, each graph has its own set of curves between ℓ and \mathcal{C}_ℓ . The schemaball thus contains all of them, which means there may be curves between the same value of ℓ and several \mathcal{C}_ℓ (and vice versa). For instance, in Fig. 5a showing the schemaball for $N = 12$ and $k = 3$, we see that for $\ell = 3$, which is cycles of length 3, also known as triangle, we find connection to $\mathcal{C}_3(12, 3) = (2, 3, 4, 5)$. This means each of the $\#\sigma_{max} = 4$ graphs has triangle, one has 2 of them, another one has 3, still another one has 4 and the final one has 5 triangle.

From the visualization using a schemaball it can be immediately seen that for $N = 12$ and $k = 3$ small cycles lengths, that is $\ell = \{3, 4, \dots, 7\}$, have generally a count $\mathcal{C}_\ell(12, 3) > 0$. For large cycle lengths, that is $\ell = \{8, 9, \dots, 12\}$, we have $\mathcal{C}_\ell(12, 3) = 0$. For $N = 14$ and $k = 3$, see Fig. 5c, we get very similar results. By contrast, for larger k , not only the cycle count $\mathcal{C}_\ell(N, k)$ is much higher than for lower k , but also the distribution over cycles lengths ℓ is quite different, see the examples $N = 12, k = 8$, Fig. 5b and $N = 14, k = 10$, Fig. 5d. Here, small as well as large cycle lengths ℓ have a substantial count $\mathcal{C}_\ell(N, k)$. Moreover, every cycles length ℓ is connected to a distinct interval of $\mathcal{C}_\ell(N, k)$. This means that the σ_{max} -graphs have very similar counts $\mathcal{C}_\ell(N, k)$ for each ℓ . These properties becomes even more clear if we additionally consider the schemaballs for σ_{min} -graphs, which are the graphs with minimal structure coefficients see Fig. 6 for the same examples as Fig. 5. Not only there are more σ_{min} -graphs than σ_{max} -graphs, (for instance 77 vs. 4 for $N = 12, k = 3$, or 359 vs. 6 for $N = 12, k = 8$), the balls for small k look very different, compare Figs. 6a and 6c with Figs. 5a and 5c. For the σ_{min} -graphs and small k even large cycle length ℓ have a substantial count $\mathcal{C}_\ell(N, k)$. The count is actually much higher, which means that σ_{min} -graphs have generally more cycles of a given length than σ_{max} -graphs. On the other hand, for large k the differences are rather marginal. The only difference is that the schemaballs are more dense, which means that σ_{min} -graphs have more different counts for a given cycle length than σ_{max} -graphs. For the other tested number of players $N \leq 14$ similar results are obtained as shown in Figs. 5 and 6. We next discuss some implications of these results on the evolution of cooperation on regular evolutionary graphs.

3 Discussion and Conclusions

In this paper structure coefficients $\sigma(\pi, \mathcal{G})$ introduced by Chen et al. [6] (see [27, 28] for further analysis) are studied for all regular interaction graphs with $N \leq 14$ players and $3 \leq k \leq N - 3$ coplayers. These structure coefficients provide a simple condition connecting long-term prevalence of cooperation with the values of the payoff matrix (4), the structure of the evolutionary graph \mathcal{G} and the arrangement of any number of cooperators and defectors on this graph, which is expressed by the configuration π . Cooperation is favored for weak selection and a configuration π on a graph \mathcal{G} if

$$\sigma(\pi, \mathcal{G}) > \frac{c - b}{a - d}. \quad (3)$$

For $\sigma(\pi, \mathcal{G}) < 1$, the game favors the evolution of spite, which can be seen as a sharp opposite to cooperation. For $\sigma(\pi, \mathcal{G}) = 1$, the condition (3) matches the standard condition of risk-dominance. For $\sigma(\pi, \mathcal{G}) > 1$, the

diagonal elements of the payoff matrix (4), a and d , are more critical than the off-diagonal elements, b and c , for determining which strategy is favored. For instance, cooperation can be favored in the Prisoner's Dilemma game, which is specified by $c > a > d > b$. The condition (3) implies that a larger value of $\sigma(\pi, \mathcal{G})$ still allows cooperation to emerge if $a - d$ is small (or $c - b$ is large). For the Stag Hunt game (Coordination game), characterized by $a > c \geq d > b$, the condition $\sigma(\pi, \mathcal{G}) > 1$ means to favor a Pareto-efficient strategy ($a > d$) over a risk-dominant strategy ($a + b < c + d$). Again, a larger value of $\sigma(\pi, \mathcal{G})$ tolerates a smaller Pareto-efficiency $a - d$. Put differently, cooperation is favored even if the difference between reward and punishment is rather low. A generalization of these discussions can be achieved by the universal scaling approach for payoff matrices that facilitates studying a continuum of social dilemmas [34]. According to this approach a larger value of $\sigma(\pi, \mathcal{G})$ implies a larger section of the parameter space spanned by gamble-intending and risk-averting dilemma strength [29]. Based on this interpretation of the structure coefficient $\sigma(\pi, \mathcal{G})$, we review the following major results of the numerical experiments presented in Sec. 2.

- a. There is an approximately linear relationship between maximal structure coefficients and the count of cycles of the interaction graph with certain length. Moreover, the number of σ_{max} -graphs grows much slower for a rising number of players than the number of k -regular graphs on N vertices. Thus, graphs with maximal structure coefficients get rare for the number of players N getting large.
- b. The values of the structure coefficients are larger for a small number of coplayers, that is for graphs with a small degree, and maximal for $k = 3$, which is cubic graphs, than for larger numbers of coplayers. This is also the case for the largest difference between maximal and minimal structure coefficients. Thus, for regular evolutionary graphs describing the interactions between players, the results for $N \leq 14$ players suggest that a smaller number of coplayers is particularly prone to promote cooperation if a favorable graph is selected. The selection of graphs does matter less for a larger number of coplayers. The σ_{max} -graphs with small numbers of coplayers k not only have largest maximal structure coefficients, they are also characterized by the absence of cycles with a length above a certain limit, see examples in the collection of σ_{max} -graphs in Appendix 3.
- c. There are not only no long cycles in σ_{max} -graphs with small k . The graphs are also structured into blocks that are connected by cut vertices and/or hinge vertices. A cut vertex is a vertex whose removal disconnects the graph, while a hinge vertex is a vertex whose removal makes the distance longer between at least two other vertices of the graphs [5, 11]. For instance, for $N = 12$ and $k = 3$, the vertices occupied by the players \mathcal{I}_3 and \mathcal{I}_9 , see Fig. 11, are cut vertices, while for $N = 10$ and $k = 4$, see Fig. 10b, the vertices occupied by the players \mathcal{I}_5 and \mathcal{I}_6 are hinge vertices as their removal would make the distance between \mathcal{I}_4 and \mathcal{I}_7 longer. The blocks are occupied by clusters of cooperators. The clusters can be seen as to serve as a mutant family that invades the remaining graph. As vertices with players of opposing strategies are connected by cut and/or hinge vertices there is only a small number of (or even just a single) migration path for the cooperators and/or defectors. A similar observation has been reported for evolutionary games on lattices grids [8, 14], see also the discussion in Sec. 2.2. To summarize: the results suggest that σ_{max} -graphs for small numbers of coplayers have some distinct graph-theoretical properties. Searching for these properties in a given graph may inform the design of interactions graphs that are either particularly prone to cooperation or particularly opposed to it.
- d. The property of missing long cycles is also a possible explanation as to why regular graphs with small degree differ substantially from graphs with larger degree in terms of promoting cooperation in

evolutionary games. A larger degree makes it impossible to have blocks that are connected by only a few edges. As the number of edges increases linearly with the degree by $kN/2$ and each vertex has the same number of edges, there is an ample supply on connections. These results imply that connectivity properties of the interaction graph play an important role in the emergence of cooperation. It may be interesting to see if these connectivity issues may possibly also show in algebraic graph measures, for instance algebraic connectivity expressed by the Fiedler vector.

The results given above show a clear dependency between the long-term prevalence of cooperation in evolutionary games on regular graphs and some of their graph-theoretical properties, which generally confirm previous findings on clusters of cooperators in games on lattice grids [8, 9, 14, 23], on pairs of mutants on a circle graph ($k = 2$) [36], and on short cooperator path lengths on some selected regular graphs with $N = 12$ and $k = 3$, among them the Frucht, the Tietze and the Franklin graph [28]. However, apart from statements about the prevalence of cooperation there are also other quantifiers of evolutionary dynamics that are highly relevant. In other words, some of the difficulty in the given approach for evaluating the emergence of cooperation in evolutionary games on graphs arises from structure coefficients merely treating a comparison of fixation probabilities. The condition indicates that the fixation probability of cooperation is higher than the fixation probability of defection. This, however, does not entail the values of these probabilities. However, structure coefficients can be calculated with polynomial time complexity [6], while computing fixation probabilities is generally intractable due to an exponential time complexity [10, 12, 33]. In other words, by using the approach involving structure coefficients, we exchange computational tractability by obtaining just a comparison of fixation probabilities instead of their exact values. Moreover, apart from the difference in the information obtained, the variety in the descriptive power of the structure coefficients as compared to the fixation probabilities is salient in another way. Most likely, there is a rather complex relationship between structure coefficients and fixation probability, which is illustrated by the example of a single cooperator for which the structure coefficient does precisely not imply unique values of the fixation probability of cooperation. For a single cooperator we get a single value of the structure coefficient, but fixation probabilities vary over initial configurations as shown for the Frucht and for the Tietze graph [16].

All these considerations show that calculating fixation probabilities and fixation times for multiple mutant configurations is not only computationally expensive, but also has a huge number of possible setups, for instance, which one of the considerable number of graphs to analyze, or where to place cooperators on the evolutionary graph and how many. There are various experimental parameters to be taken into account, which might be why so far systematically conducted numerical studies are sparse. In this sense, another contribution of this paper might be seen in pointing at settings for numerical experiments calculating fixation probabilities and fixation times. The results given in this paper show that among all the regular interaction graphs with $N \leq 14$ players and $3 \leq k \leq N - 3$ coplayers, there is a comparably small number of graphs (as given in Tab. 1) which favor cooperation more than others. It may be interesting to see if these graphs also stand out in terms of fixation probability and fixation time as compared to a graph randomly drawn from the other ones.

Acknowledgments:

I wish to thank Markus Meringer for making available the `genreg` software [17] used for generating the regular graphs according to Tab. 2 and for helpful discussions.

Appendix A Configurations, regular graphs and structure coefficients

The co-evolutionary games we consider here have N players $\mathcal{I} = \{\mathcal{I}_i\}$, $i = 1, 2, \dots, N$, that each uses either of two strategies $\pi_i \in \{C, D\}$, which we may interpret as cooperating or defecting. Each player \mathcal{I}_i , which interacts with a coplayer \mathcal{I}_j , receives payoff according to the 2×2 payoff matrix

$$\begin{array}{c|cc} i \setminus j & C & D \\ \hline C & (a & b) \\ D & (c & d) \end{array}. \quad (4)$$

Which player interacts with whom is described by the interaction graph $\mathcal{G} = (V, E)$, where the vertices $v_i \in V$ represent the players and the edges $e_{ij} \in E$ indicate that the players \mathcal{I}_i and \mathcal{I}_j interact as mutual coplayers [15, 22, 26]. Which strategy is used by which player at a given point of time is specified by a configuration $\pi = (\pi_1, \pi_2, \dots, \pi_N)$ with $\pi_i \in \{C, D\}$. If we represent the two strategies by a binary code $\{C, D\} \rightarrow \{1, 0\}$, a configuration appears as a binary string the Hamming weight of which denotes the number of cooperators $c(\pi)$. For games with N players, there are 2^N configurations with 2 configurations ($\pi = (00 \dots 0)$ and $\pi = (11 \dots 1)$) absorbing. Players may update their strategies in an updating process, for instance death–birth (DB) or birth–death (BD) updating [1, 24]. Recently, it was shown by Chen et al. [6] that strategy $\pi_i = 1 = C$ is favored over $\pi_i = 0 = D$ if

$$\sigma(\pi, \mathcal{G})(a - d) > (c - b). \quad (5)$$

This results applies to weak selection and 2×2 games with N players, payoff matrix (4), any configuration π of cooperators and defectors and for any interaction network modeled by a simple, connected, k -regular graph.

The quantity $\sigma(\pi, \mathcal{G})$ in Eq. (5) is the structure coefficient of the configuration π and the graph \mathcal{G} . It may not have the same value for different arrangements of cooperators and defectors described by the configuration π and also for different interaction networks modeled by a regular graph \mathcal{G} . In particular, it was shown that for weak selection and the graph \mathcal{G} describing interaction as well as replacement graph, the structure coefficient $\sigma(\pi, \mathcal{G})$ can be calculated with time complexity $\mathcal{O}(k^2 N)$ for DB and BD updating [6]. For DB updating there is

$$\sigma(\pi, \mathcal{G}) = \frac{N(1 + 1/k)\overline{\omega^1} \cdot \overline{\omega^0} - 2\overline{\omega^{10}} - \overline{\omega^1 \omega^0}}{N(1 - 1/k)\overline{\omega^1} \cdot \overline{\omega^0} + \overline{\omega^1 \omega^0}}, \quad (6)$$

with 4 local frequencies ($\overline{\omega^1}$, $\overline{\omega^0}$, $\overline{\omega^{10}}$ and $\overline{\omega^1 \omega^0}$), which depend on π and \mathcal{G} , see [6, 27, 28] for a probabilistic interpretation of these frequencies. Our focus here is on DB updating as it has been shown that BD updating never favors cooperation [6].

Appendix B Isomorphic graphs, isomorphic configurations and cycle counts

The structure coefficient $\sigma(\pi, \mathcal{G})$, as for instance defined for DB updating by Eq. (6), may vary over configurations π and graphs \mathcal{G} . This suggests the question of upper and lower bounds of $\sigma(\pi, \mathcal{G})$. For a rather low number of players it appears feasible to check all $\sigma(\pi, \mathcal{G})$, as demonstrated in the paper for $N \leq 14$ and all regular graphs with up to 14 vertices. For a 2×2 game with N players, there are $2^N - 2$ non-absorbing configurations π . These configurations can be grouped according to the number of cooperators

Table 2: The numbers $\mathcal{L}_k(N)$ of simple connected k -regular graphs on N vertices, [17], which corresponds to the number of regular interaction graphs with N players and k coplayers for $6 \leq N \leq 14$ and $3 \leq k \leq N - 1$. Note that there is more than one graph, $\mathcal{L}_k(N) > 1$, only for $k \leq N - 3$.

$k \setminus N$	6	7	8	9	10	11	12	13	14
3	2	0	5	0	19	0	85	0	509
4	1	2	6	16	59	265	1.544	10.778	88.168
5	1	0	3	0	60	0	7.848	0	3.459.383
6	0	1	1	4	21	266	7.849	367.860	21.609.300
7	0	0	1	0	5	0	1.547	0	21.609.301
8	0	0	0	1	1	6	94	10.786	3.459.386
9	0	0	0	0	1	0	9	0	88.193
10	0	0	0	0	0	1	1	10	540
11	0	0	0	0	0	0	1	0	13
12	0	0	0	0	0	0	0	1	1
13	0	0	0	0	0	0	0	0	1

$c(\pi)$, $2 \leq c(\pi) \leq N - 2$. The number of simple, connected regular graphs is known for small numbers of vertices, e.g. [17], see Tab. 2. Note that these numbers apply to graphs that are all not isomorphic with each isomorphism class being represented by exactly one graph. In other words, Tab. 2 also gives the number of isomorphism classes for all $6 \leq N \leq 14$ and $3 \leq k \leq N - 1$. Isomorphism refers to the property that two graphs are structurally alike and merely differ in how the vertices and edges are named. More precisely, two graphs are isomorphic if there is a bijective mapping θ between their vertices which preserves adjacency [3], pp. 12–14.

Consider, for example, the $\mathcal{L}_3(6) = 2$ interaction graphs with $N = 6$ players, each with $k = 3$ coplayers, see Fig. 7. For the graph in Fig. 7a we get the maximal structure coefficient $\sigma_{max} = 1.1818$ for 2 configurations, $\pi = (111000)$ as shown in Fig. 7a and $\pi = (000111)$. By the isomorphism $\theta = \begin{pmatrix} v_1 & v_2 & v_3 & v_4 & v_5 & v_6 \\ 1 & 2 & 3 & 4 & 5 & 6 \\ 6 & 1 & 2 & 3 & 4 & 5 \end{pmatrix}$, we obtain an isomorphic graph as shown in Fig. 7b. For this graph, the configuration $\pi = (111000)$ has $\sigma = 1.0000$, but $\pi = (110001)$ and $\pi = (001110)$ have $\sigma_{max} = 1.1818$. Note that between the configurations with σ_{max} the same isomorphic mapping θ applies. In other words, the structure coefficients are invariant under isomorphic mappings. For each pair of isomorphic graphs, there are isomorphic configurations that have the same value of the structure coefficient. For the graph in Fig. 7c, we obtain the result that the structure coefficient is constant over all configurations (except the absorbing configurations). Thus, isomorphic transformations do not alter the values of $\sigma(\pi, \mathcal{G})$.

These results apply generally to structure coefficients $\sigma(\pi, \mathcal{G})$ of regular graphs. The local frequencies in Eq. (6) solely depend on counting two types of paths on the interaction graph [6, 27, 28]. The quantities $\overline{\omega^1}$, $\overline{\omega^0}$ and $\overline{\omega^1\omega^0}$ relate to the number of paths with length 1 that connect any vertex with adjacent vertices that hold a cooperator (or defector). The quantity $\overline{\omega^{10}}$ relates to the number of paths with length 2 from any vertex to adjacent vertices on which the first vertex of the path holds a cooperator and the second vertex holds a defector. As an isomorphic reshuffling of vertices preserves adjacency, these numbers stay the same if the isomorphism acts on both the vertices and the configurations. Thus, suppose two graphs \mathcal{G}_i and \mathcal{G}_j are isomorphic with isomorphism θ . Then, it follows $\sigma(\pi, \mathcal{G}_i) = \sigma(\theta(\pi), \mathcal{G}_j)$. Furthermore,

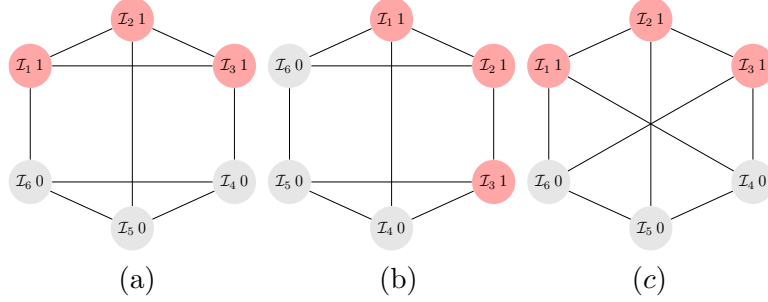


Figure 7: The $\mathcal{L}_3(6) = 2$ interaction graphs with $N = 6$ players, each with $k = 3$ copleys. All are vertex-transitive and (c) is even symmetric (edge-transitive). The graph in (a) has a maximal structure coefficient $\sigma_{max} = 1.1818$, which is obtained for two configurations with $c(\pi) = 3$ cooperators: $\pi = (111000)$ (as shown in (a)) and $\pi = (000111)$. For the isomorphic graph in (b), we get $\sigma_{max} = 1.1818$ for the isomorphic configurations $\pi = (110001)$ and $\pi = (001110)$. The graph in (c) has the same structure coefficient $\sigma = 1.0000$ for all configurations. Regarding the count of cycles with length ℓ , we see that the graphs in (a) and (b) have $\mathcal{C}_{\ell_1}(6, 3) = (2, 3, 6, 2)$, while for the graph in (c) there is $\mathcal{C}_{\ell_2}(6, 3) = (0, 9, 0, 6)$.

the maximal structure coefficient is invariant as well, that is for isomorphic graphs \mathcal{G}_i and \mathcal{G}_j there is $\sigma_{max_i} = \max_{\pi} \sigma(\pi, \mathcal{G}_i) = \sigma_{max_j} = \max_{\pi} \sigma(\pi, \mathcal{G}_j)$. Any regular graph belongs to one of the isomorphism classes and can be obtained by isomorphic transformations by any member of this class. Regular interaction graphs that are isomorphic have the same distribution of structure coefficients $\sigma(\pi, \mathcal{G})$ over the number of cooperators $c(\pi)$. Thus, by considering one representative of each isomorphism class, we can make statements about structure coefficients for all regular graphs.

For each graph, there is a specific count $\mathcal{C}_{\ell}(N, k)$ of cycles with length ℓ , $3 \leq \ell \leq N$. There are efficient algorithms to count these cycles [7]. Consider again the $\mathcal{L}_3(6) = 2$ graphs with $N = 6$ players and $k = 3$ copleys, see Fig. 7. We find the graph in Fig. 7a and Fig. 7b has $\mathcal{C}_{\ell_1}(6, 3) = (2, 3, 6, 2)$ with $\ell = \{3, 4, 5, 6\}$ (there are 2 cycles of length $\ell = 3$, 3 cycles of length $\ell = 4$, 6 cycles of length $\ell = 5$ and so on), while the graph in Fig. 7c has $\mathcal{C}_{\ell_2}(6, 3) = (0, 9, 0, 6)$. It generally applies that isomorphic graphs have the same $\mathcal{C}_{\ell}(N, k)$. Graphs that are not isomorphic have frequently a distinct count $\mathcal{C}_{\ell}(N, k)$, but there are also cases, particularly for N getting larger, where 2 not isomorphic graphs have the same count $\mathcal{C}_{\ell}(N, k)$.

Appendix C Collection of σ_{max} -graphs with $N \leq 14$

We here give a collection of selected σ_{max} -graphs with $N \leq 14$. The graphs are shown to illustrate some graph-theoretical properties associated with prevalence of cooperation. The single σ_{max} -graph with $N = 6$ is already shown in Fig. 7a. For $N = 7$, there are $\mathcal{L}_4(7) = 2$ regular graph, which both have the same maximal structure coefficients. In other words, the count of graphs equals the count of σ_{max} -graph, which is why they are not included in the collection.

Figs. 8–10 shown all σ_{max} -graphs for $N = 8, 9, 10$ and $3 \leq k \leq N - 3$ together with σ_{max} and the associated configurations. For $N = 12$ and $N = 14$, only some examples of σ_{max} -graphs are given in Figs. 11–13 due to brevity. A full list of all σ_{max} -graphs for $11 \leq N \leq 14$ and $3 \leq k \leq N - 3$ is made available here [30]. It is particularly noticeable that the σ_{max} -graphs are structured to have blocks with clusters of mutants. For instance, we see such a block with $(\mathcal{I}_1, \mathcal{I}_2, \mathcal{I}_3, \mathcal{I}_4)$ for the graph with $N = 8$ and $k = 3$ in

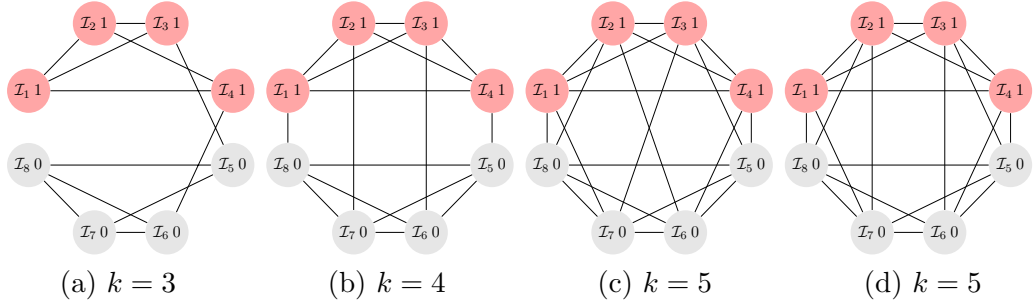


Figure 8: The σ_{max} -graphs for $N = 8$ and $k = 3, 4, 5$. We get $\sigma_{max} = 1.6538$ for $k = 3$, (a), $\sigma_{max} = 1.2222$ for $k = 4$, (b), and $\sigma_{max} = 0.9565$ for the 2 σ_{max} -graphs with $k = 5$, (c),(d), each for the configuration $\pi = (1111\ 0000)$. In addition, the same structure coefficient is obtained also for the configuration $\pi = (0000\ 1111)$, and only for (d) additionally for $\pi = (1100\ 0011)$ and $\pi = (0011\ 1100)$.

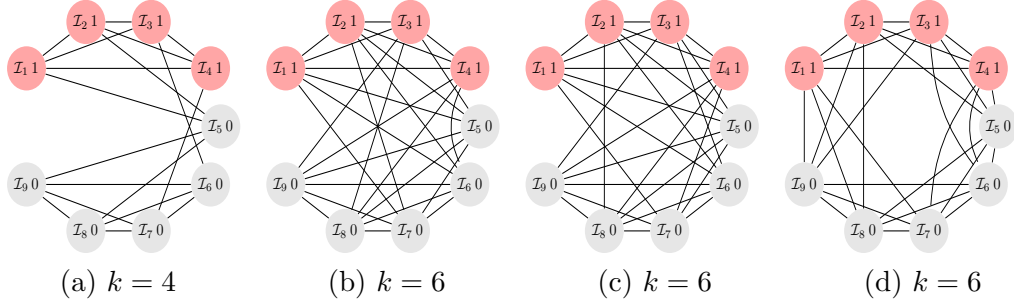


Figure 9: The σ_{max} -graphs for $N = 9$ and $k = 4, 6$. We get $\sigma_{max} = 1.3206$ for $k = 4$ (a) and the configuration $\pi = (11110\ 0000)$, but also for $\pi = (11111\ 0000)$, $\pi = (00000\ 1111)$ and $\pi = (00001\ 1111)$. For $k = 6$, there are 3 σ_{max} -graphs, (b),(c),(d), each with $\sigma_{max} = 0.9115$ for the configuration $\pi = (11110\ 0000)$. There are several more configurations that have the same σ_{max} due to the symmetry properties of these 3 graphs.

Fig. 8a and for $N = 9$ and $k = 4$ in Fig. 9a, or for $N = 10$ and $k = 3$, Fig. 10a and for the cubic graphs ($k = 3$) with $N = 12$ and $N = 14$ as well, see Figs. 11 and 13. The σ_{max} -graphs with larger degree (= coplayers) still somewhat retains such a “blockish” appearance (for instance $(\mathcal{I}_1, \mathcal{I}_2, \mathcal{I}_3, \mathcal{I}_4, \mathcal{I}_5)$ in Fig. 10c) but to a far lesser degree. In addition, σ_{max} -graphs with larger degree are frequently vertex-transitive (for instance Figs. 9d, 10e and 10g) which is not the case for cubic ($k = 3$) and quartic ($k = 4$) σ_{max} -graphs with $N \leq 14$, with the exception of $N = 6$ and $k = 3$, see Fig. 7a. Furthermore, it can be observed that the blocks are occupied by clusters of cooperators which are frequently connected by cut vertices and/or hinge vertices. For instance, for $N = 12$ and $k = 3$, the vertices occupied by the players \mathcal{I}_3 and \mathcal{I}_9 , see Fig. 11, are cut vertices, while for $N = 10$ and $k = 4$, see Fig. 10b, the vertices occupied by the players \mathcal{I}_5 and \mathcal{I}_6 are hinge vertices as their removal would make the distance between \mathcal{I}_4 and \mathcal{I}_7 longer. As discussed above, the clusters can be seen as to serve as a mutant family that invades the remaining graph. As vertices with players of opposing strategies are connected by cut and/or hinge vertices there is only a small number of (or even just a single) migration path for the cooperators and/or defectors.

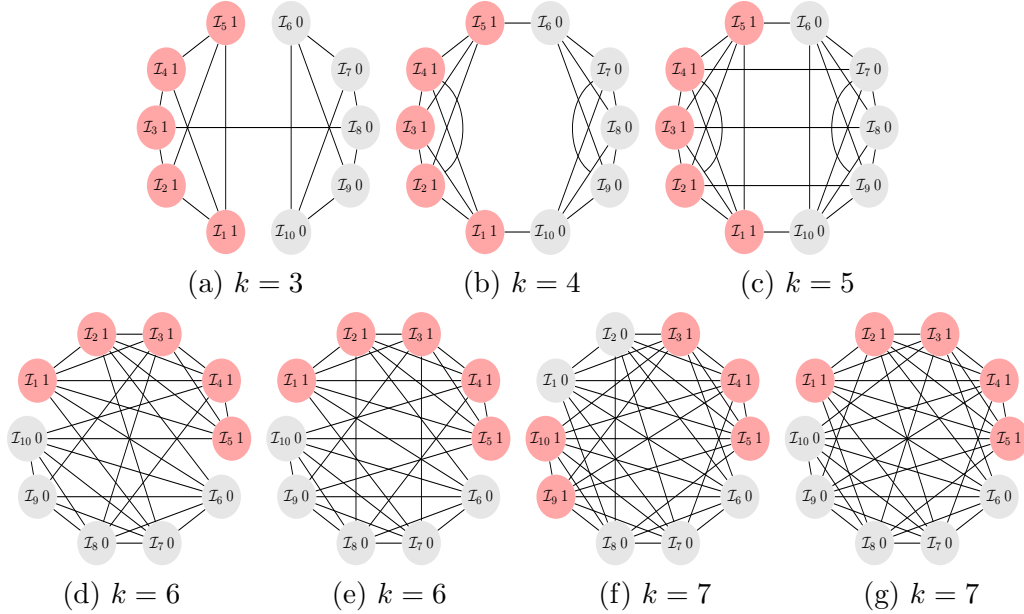


Figure 10: The σ_{max} -graphs for $N = 10$ and $k = 3, 4, \dots, 7$. We get $\sigma_{max} = 1.8831$ for $k = 3$ (a), $\sigma_{max} = 1.5128$ for $k = 4$ (b), $\sigma_{max} = 1.2222$ for $k = 5$ (c), $\sigma_{max} = 1.0241$ for $k = 6$ (d),(e) and $\sigma_{max} = 0.9145$ for $k = 7$ (f),(g), all for the configuration $\pi = (11111\ 00000)$, and also for $\pi = (00000\ 11111)$. For one graph with $k = 7$,(f) the maximal structure coefficient is also obtained for 2 more configurations.

References

- [1] Allen, B., Nowak, M. A., 2014. Games on graphs. EMS Surv. Math. Sci. 1, 113–151.
- [2] Allen, B., Lippner, G., Chen, Y. T., Fotouhi, B., Momeni, N., Yau, S. T., Nowak, M. A., 2017. Evolutionary dynamics on any population structure. Nature 544, 227–230.
- [3] Bondy, J. A., Murty, U. S. R., 2008. Graph Theory, Springer, Berlin.
- [4] Broom, M., Rychtar, J., 2013. Game-Theoretical Models in Biology. Chapman and Hall/CRC, Boca Raton, FL, USA.
- [5] Chang, J. M., Hsu, C. C., Wang, Y. L., Ho, T. Y., 1997. Finding the set of all hinge vertices for strongly chordal graphs in linear time. Information Sciences 99, 173–182.
- [6] Chen, Y. T., McAvoy, A., Nowak, M. A., 2016. Fixation probabilities for any configuration of two strategies on regular graphs. Sci. Rep. 6, 39181.
- [7] Giscard, P. L., Kriege, N., Wilson, R. C., 2019. A general purpose algorithm for counting simple cycles and simple paths of any length. Algorithmica 81, 2716–2737.
- [8] Hauert, C., 2001. Fundamental clusters in spatial 2×2 games. Proc. Roy. Soc. B268, 761–769.
- [9] Hauert, C., Doebeli, M. 2004. Spatial structure often inhibits the evolution of cooperation in the snowdrift game. Nature 428, 643–646.

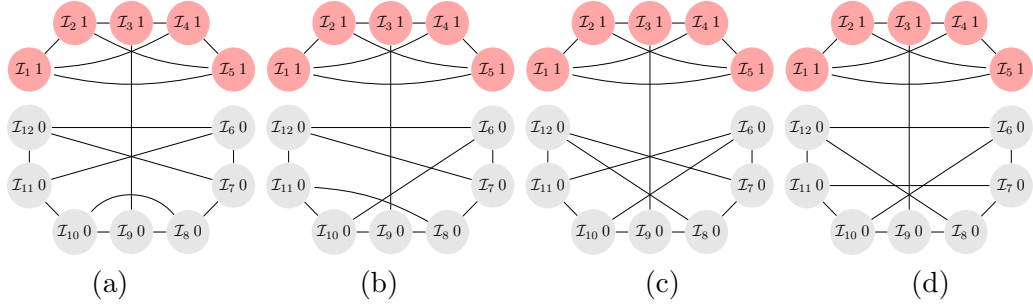


Figure 11: The σ_{max} -graphs for $N = 12$ and $k = 3$, each with $\sigma_{max} = 1.9159$ for the configuration $\pi = (111110000000)$ (and also for $\pi = (0000\ 0111\ 1111)$).

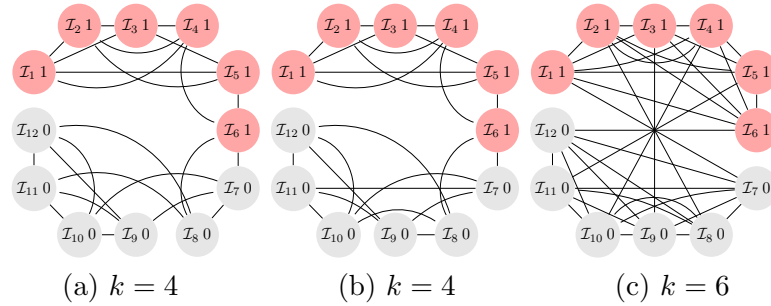


Figure 12: The σ_{max} -graphs for $N = 12$ and $k = 4, 6$. We have $\sigma_{max} = 1.5701$ for $k = 4$ (a),(b) and $\sigma_{max} = 1.2105$ for $k = 6$ (c), each for the configuration $\pi = (1111\ 1100\ 0000)$ (and also for $\pi = (0000\ 0011\ 1111)$).

[10] Hindersin, L., Möller, M., Traulsen, A., Bauer, B., 2016. Exact numerical calculation of fixation probability and time on graphs. *BioSystems* 150, 87–91.

[11] Ho, T. Y., Wang, Y. L., Juan, M. T., 1996. A linear time algorithm for finding all hinge vertices of a permutation graph. *Information Processing Letters* 59, 103–107.

[12] Ibsen-Jensen, R., Chatterjee, K., Nowak, M. A., 2015. Computational complexity of ecological and evolutionary spatial dynamics. *Proc. Natl. Acad. Sci. U.S.A.* 112, 15636–15641.

[13] Krzywinski, M., 2004. Schemaball: A new spin on database visualization. *SysAdmin Magazine* 13, 23–28.

[14] Langer, P., Nowak, M. A., Hauert, C., 2008. Spatial invasion of cooperation. *J. Theor. Biol.* 250, 634–641.

[15] Lieberman, E., Hauert, C., Nowak, M. A., 2005. Evolutionary dynamics on graphs. *Nature* 433, 312–316.

[16] McAvoy, A., Hauert, C., 2015. Structural symmetry in evolutionary games. *J. R. Soc. Interface* 12, 20150420.

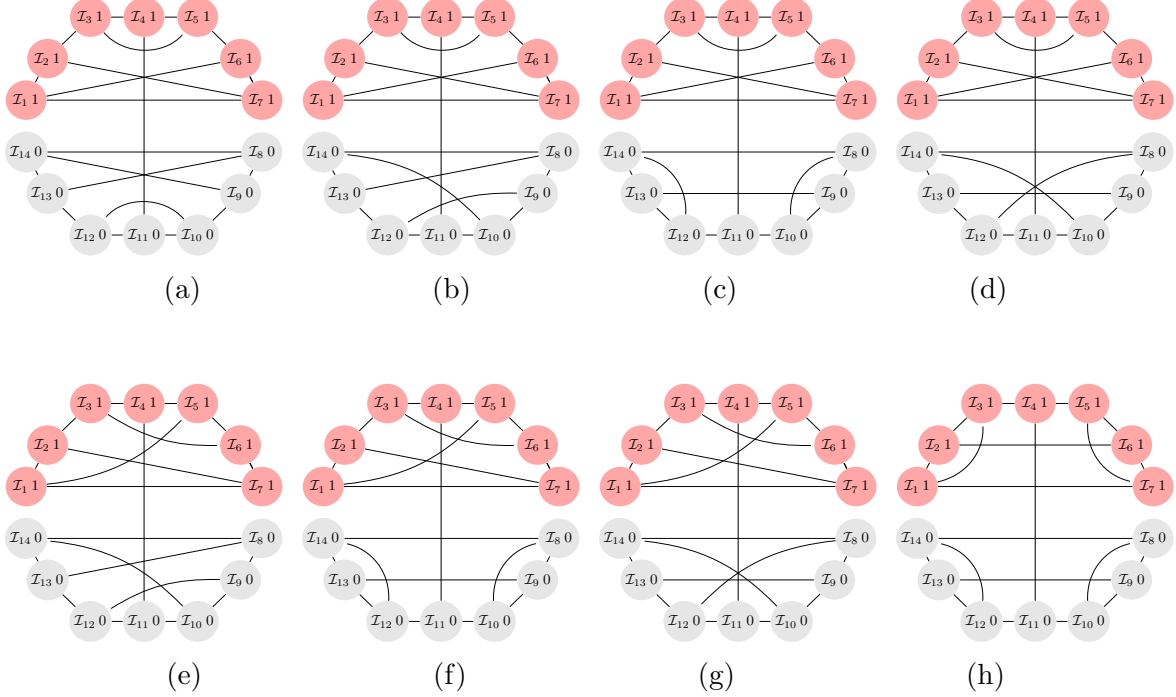


Figure 13: The σ_{max} -graphs for $N = 14$ and $k = 3$, each with $\sigma_{max} = 1.9396$ for the configuration $\pi = (1111\ 1110\ 0000\ 00)$ (and also for $\pi = (0000\ 0001\ 1111\ 11)$). Only 8 out of $\#_{sigma_{max}} = 10$ σ_{max} -graphs according to Tab. 1 are depicted. The remaining 2 graphs arise from the blocks depicted in the figures. If we call the upper half of the graphs in Fig. 13 (a)–(d) the A-block, then the lower half of these graphs consists of blocks A, B, C and D. The blocks are joined by the edge connecting \mathcal{I}_4 and \mathcal{I}_{11} . The graphs in 13 (e)–(f) also are block-like with blocks B–B, B–C, B–D and C–C. The 2 remaining graphs are formed by connecting the blocks C–D and D–D.

- [17] Meringer, M., 1999. Fast generation of regular graphs and construction of cages. *J. Graph Theory* 30, 137–146.
- [18] Möller, M., Hindersin, L., Traulsen, A., 2019. Exploring and mapping the universe of evolutionary graphs identifies structural properties affecting fixation probability and time. *Commun. Biol.* 2–137.
- [19] Newton, J., 2018. Evolutionary game theory: A renaissance. *Games* 9(2), 31.
- [20] Nowak, M. A., 2006. *Evolutionary Dynamics: Exploring the Equations of Life*. Harvard University Press, Cambridge, MA.
- [21] Ohtsuki, H., Hauert, C., Lieberman, E., Nowak, M. A., 2006. A simple rule for the evolution of cooperation on graphs and social networks. *Nature* 441, 502–505.
- [22] Ohtsuki, H., Pacheco, J. M., Nowak, M. A., 2007. Evolutionary graph theory: Breaking the symmetry between interaction and replacement. *J. Theor. Biol.* 246, 681–694.

- [23] Page, K. M., Nowak, M. A., Sigmund, K., 2000. The spatial ultimatum game. *Proc. Roy. Soc.* B267, 2177–2182.
- [24] Pattni, K., Broom, M., Silvers, L., Rychtar, J., 2015. Evolutionary graph theory revisited: When is an evolutionary process equivalent to the Moran process? *Proc. Roy. Soc.* A471 20150334.
- [25] Pavlogiannis, A., Tkadlec, J., Chatterjee, K., Nowak, M. A., 2018. Construction of arbitrarily strong amplifiers of natural selection using evolutionary graph theory. *Commun. Biol.* 1–71.
- [26] Richter, H., 2017. Dynamic landscape models of coevolutionary games. *BioSystems* 153–154, 26–44.
- [27] Richter, H., 2019. Properties of network structures, structure coefficients, and benefit-to-cost ratios. *BioSystems* 180, 88–100.
- [28] Richter, H., 2019. Fixation properties of multiple cooperator configurations on regular graphs. *Theory in Biosciences* 138, 261–275.
- [29] Richter, H., 2020. Relationships between dilemma strength and fixation properties in coevolutionary games. In: Liu, Y., Wang, L., Zhao, L., Yu, Z. (Eds.) *Advances in Natural Computation, Fuzzy Systems and Knowledge Discovery. Advances in Intelligent Systems and Computing*, Vol 1074, Springer Nature, 252–259.
- [30] <https://github.com/HendrikRichterLeipzig/StructureCoefficientsRegularGraphs>
- [31] Tarnita, C. E., Ohtsuki, H., Antal, T., Fu, F., Nowak, M. A., 2009. Strategy selection in structured populations. *J. Theor. Biol.* 259, 570–581.
- [32] Tkadlec, J., Pavlogiannis, A., Chatterjee, K., Nowak, M. A., 2019. Population structure determines the tradeoff between fixation probability and fixation time. *Commun. Biol.* 2–138.
- [33] Voorhees, B., 2013. Birth–death fixation probabilities for structured populations. *Proc. Roy. Soc.* A469, 20120248.
- [34] Wang, Z., Kokubo, S., Jusup, M., Tanimoto, J., 2015. Universal scaling for the dilemma strength in evolutionary games. *Phys. Life Rev.* 14, 1–30.
- [35] Wu, B., Traulsen, A., Gokhale, C. S., 2013. Dynamic properties of evolutionary multi–player games in finite populations. *Games* 4, 182–199.
- [36] Xiao, Y, Wu, B., 2019. Close spatial arrangement of mutants favors and disfavors fixation. *PLoS Comput Biol.* 15(9): e1007212.